

# Classifying Morphologically Similar Tree Species in Central European Forests Using Geometric Bark-Structure Features Derived from Terrestrial Laser Scanning

Marie Weber<sup>1</sup>, Katja Richter<sup>1</sup> & Anne Bienert<sup>1</sup>

## Abstract

Increasing digitalization in forest monitoring, often summarized under the concept of *Forest 4.0*, has accelerated the use of terrestrial, mobile, and UAV-borne LiDAR systems for large-scale forest inventory assessments. While ground-based LiDAR-derived 3D point clouds reliably support the extraction of structural parameters such as diameter at breast height (DBH) and crown volume, accurate species identification remains a significant challenge - particularly for morphologically similar species that are difficult to distinguish due to their external appearance or structural characteristics. This study focuses on the distinction between European hornbeam (*Carpinus betulus L.*), European beech (*Fagus sylvatica L.*) and Pedunculate Oak (*Quercus robur L.*), as conventional automatically derived features such as branching patterns and diameter ratios at various structure points alone struggle to satisfy the accuracy requirements of classification algorithms. This work aims to derive additional features from bark structure for potential use in terrestrial laser scanning (TLS) based species classification. For this purpose, we propose a workflow to extract bark structure features from TLS point cloud data. The first step includes the reduction to a stem section from full tree point clouds and the removal of branches as well as noise. In the second step, standard geometric surface descriptors (e.g., planarity, sphericity, and related scale-dependent features) are derived for each stem section. Initial findings indicate that bark-related geometric features can be successfully retrieved from LiDAR data, suggesting potential discriminative power at species level. However, several challenges remain, including variations in point-density across platforms, and the age-dependent nature of bark roughness. Despite these uncertainties, this study provides a promising basis for enhanced species classification in Central European forests. By enabling finer distinctions between highly similar tree species, this work contributes to improved automation in forest inventories, supports climate-adaptation strategies, and highlights the value of detailed bark-level information within digital forestry workflows.

**Keywords** tree species classification · forest inventory · terrestrial laser scanning · geometric bark features

## 1 Introduction

Forest management is undergoing rapid transformations due to the integration of digital technologies, automation and climate-smart forestry, a transformation often summarized as “Forest 4.0” (Wang et al., 2024; Ehrlich-Sommer et al., 2024; Damaševičius et al., 2024). Forest inventory is just one of many examples in which classical in-situ processes are increasingly replaced by digital and automated workflows, driven by the need for objective, repetitive and detailed monitoring. Geospatial technologies such as laser scanning present a reliable approach to acquire large scale data and inventory (Mahabir & Shrestha, 2015; Liang et al., 2016).

The changing temperatures, precipitation patterns and other meteorologically driven phenomena permanently alter

species distribution, forest vitality and competitive balance (Morin et al., 2018). These dynamic and long-term changes challenge traditional forest assessments and therefore require monitoring approaches that capture both shifts in species composition and the development of existing species, especially in natural forests where human intervention is kept at a minimum.

Airborne, mobile and terrestrial laser scanning data has been widely used for automated tree species classification, predominantly relying on crown structure, stem geometry and intensity- or waveform-derived features (Li et al., 2013; Koenig & Höfle, 2016; Michałowska & Rapiński, 2021). Where traditional inventory can rely on details such as leaf shape and structure, coloration and seasonal phenology, LiDAR driven approaches can fail to capture these qualities due to limited resolution, meteorological constraints and chosen method of acquisition. In addition, species found in

<sup>1</sup> Dresden University of Technology, Institute of Photogrammetry and Remote Sensing, Helmholtzstraße 10, D-01069 Dresden, E-Mail: marie.weber1@mailbox.tu-dresden.de

Central European deciduous forests tend to exhibit similar crown structure and comparable stem-branch geometries, leading to issues with the consistent and reliable identification of species.

This is further supported by an unpublished preliminary study we conducted, in which we used a Random Forest (RF) approach to classify pedunculate oak, European hornbeam, and European beech based on architectural metrics. However, tree species whose crown structures differ very little can nevertheless exhibit significant differences in their bark structure. It could therefore serve as an additional feature in classification but is rarely exploited in TLS-based species classification (Meng et al., 2024). From a geometric perspective, bark texture manifests as local surface roughness and curvature variation.

This contribution presents a comprehensive workflow for the extraction of bark structure from TLS point clouds by segmenting stem sections and computing multi-scale geometric surface features as presented by Weinmann et al. (2015) and Hackel et al. (2016). For further processing, the point-based results are aggregated into tree-level metrics. In a final step, the feature set is reduced by correlation-based clustering. While the initial aim of the work is to derive a metric capable of automatically distinguishing between European hornbeam and beech, the Pedunculate oak was processed alongside to work as proof of concept, as it exhibits the same features in a more pronounced manner.

## 2 Materials and Methods

To assess the value of bark structure in tree species classification, a study was conducted in a Central European forest. Section 2.1 describes the study area and the collected TLS data. Section 2.2 provides an overview of the proposed workflow and the structure of the subsequent subsections.

### 2.1 Study Area and Data

The processed TLS data sets were obtained during a survey campaign in the Lauerholz (53° 53' 2" N, 10° 44' 11" E), a deciduous forest covering almost 880 ha in northern Germany near Lübeck. The data acquisition was carried out in March 2017 with the Riegl VZ-400i laser scanner. A raster grid survey design was developed, ensuring that each inventory plot was covered from five positions – one in the middle and the four compass directions respectively, with a maximum of 25 m in between. An angular resolution of 0.04° was set. The laser footprint is given as 5.2 mm at 15 m scanning distance. This approach leads to full, but uneven coverage. The point spacing varies strongly per tree due to

occlusion and scanning distances. For further processing, the individual trees were segmented from the fully registered plots, cleaned and assigned a unique identification number as well as a species label. Basic inventory parameters such as DBH, tree position and tree height were automatically determined in an earlier automatic inventory (Bienert et al., 2021). In the nine plots studied here, eight tree species were present. We concentrated on the three most common ones: Pedunculate Oak (*Quercus robur* L.), European hornbeam (*Carpinus betulus* L.) and European beech (*Fagus sylvatica* L.), with a focus on distinguishing between the latter two.

### 2.2 Overview of the Proposed Workflow

Figure 1 provides an overview of the basic procedure of the proposed workflow for deriving bark structure parameters. The workflow starts with the individually segmented tree point clouds. To reduce a tree to its bark quality, a section with reliable straightness and minimal branching must be extracted (Sec. 2.3). This is done by performing a vertical slice at breast height (1.30 m), applying a radial crop based on the DBH and excluding branch points based on verticality metrics. Because of the uneven point spacing and remaining noise, a density filter is implemented as the final part of the stem extraction. The second step consists of deriving the geometric features using several radii (Sec. 2.4). Thresholds are implemented to ensure the tree data reaches minimum quality standards. As each feature is computed for every single point of the cloud, summarizing metrics such as mean, median and quartile range are calculated after the values pass through a light outlier filter. The resulting scalars are added as features to the data frame and later assessed for their usability on distinguishing species (Sec. 2.5). The result is a compact and consistent data frame with the most distinctive features for every processed tree.

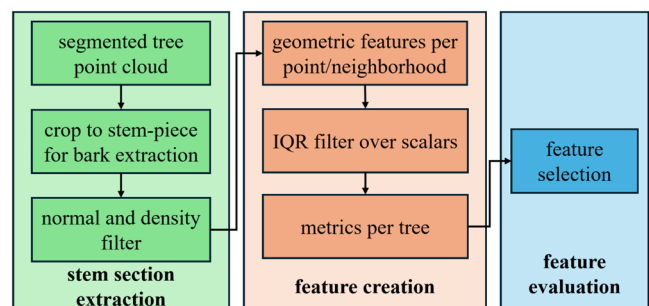


**Figure 1** The general workflow, divided into stem section extraction, feature creation and feature evaluation

## 2.3 Stem Section Extraction

The individual steps of stem extraction are shown in Figure 2. At first, we extracted a 50 cm vertical slice by extending 25 cm above and below the designated breast height, to prevent interference from branches, occlusion or uneven point spacing in the workflow performance (see Fig. 2, z-crop). This provides enough points for the following operations. To crop out any remaining branches, a radius filter was applied, masking out all points further from the DBH center coordinate than half the DBH, plus a buffer of 5 cm (see Fig. 2, hz-crop). The buffer was not installed to counteract mismeasurements of the DBH coordinate or measurement, but to account for the slight skewness most trees have. Although the horizontal crop cuts as close to the tree as possible, parts of the branches may remain. Thus, a Principal Component Analysis (PCA) based normal filter was installed to further filter out branch points (see Fig. 2, normal filter). The eigenvector associated with the smallest eigenvalue approximates the local surface normal direction. As trees can be assumed to be nearly vertical cylinders at the given height, normals should be orthogonal to the tree stem. Because branch geometry does not follow this assumption, we retained only those points whose normal vectors had a vertical component exceeding a verticality threshold of  $75^\circ$ .

In addition to possibly remaining branch points, the structure of bark itself is prone to higher noise levels, especially if overgrown or rough. As the scanning distance varied between decimeters and several dozen meters, point spacing, coverage and overlap show high variations as well. In order to produce reliable and consistent results, this was taken into account by adding a density filter as the last geometric filtering operator (see Fig. 2 density filter). This ensures that a minimum number of points per area exists to capture the bark's structure. The neighboring points of each point within a radius of 2.5 cm were extracted. If their number exceeds 20 points, the center point is retained; otherwise, the point is eliminated. Especially in cases where the tree trunk is made up of various registered point clouds, this can lead to the elimination of parts with low density due to high scanning distance, while maintaining the parts with adequate capture of structure.

Various parameter combinations were tested empirically on an exemplary set of trees of different point densities and noise levels. Figure 3 shows an example of noise which can be attributed to neither bark, branches nor the usual pattern of registration errors. The presented parameter combination has proven to achieve the best trade-off between point elimination where necessary and retaining enough

information for the following bark analysis across point cloud qualities.

A minimum threshold of 1,000 points was required for a stem section to be retained for further processing, ensuring sufficient point density and coherency for meaningful geometric analysis.

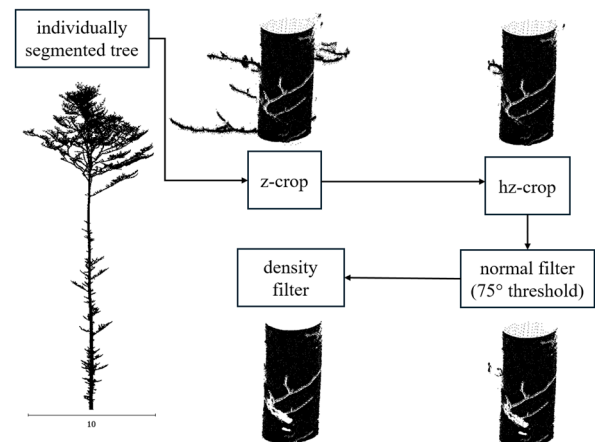


**Figure 2** The steps of stem extraction performed on a European beech. Z-crop refers to the vertical stem slice, hz-crop to the radial filter in the xy-direction

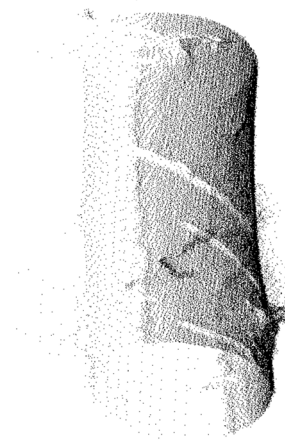


**Figure 3** A European beech showing occlusion, uneven point density and noise – all of which can hinder or distort features. (Tree section is shown after vertical and radial cropping, before normal- and density-based filtering)

## 2.4 Derivation of Geometric Features

### 2.4.1 Geometric Features

For each point of a stem section, the geometric features proposed by Weinmann et al. (2015) were computed across different scales. For this purpose, local covariance matrices were computed within radius of 1 cm, 3 cm and 5 cm respectively around each point. From these, the three

eigenvalues ( $\lambda_1$ ,  $\lambda_2$ ,  $\lambda_3$ ) were derived. Subsequently, geometric features including the sum of eigenvalues, omnivariance, eigenentropy, anisotropy, planarity, linearity, surface variance and sphericity were calculated.

Eigenvalues describe the variance of points along the three principal directions of the local point distribution. The largest eigenvalue  $\lambda_1$  reflects variation along the dominant structural direction, while  $\lambda_2$  captures variation along the secondary surface direction and  $\lambda_3$  represents variation orthogonal to the local surface. For a cylindrical stem, this results in  $\lambda_3 \ll \lambda_2 \approx \lambda_1$ . As the general pattern is distinct, smaller patterns and structures such as bark detail can be encapsulated in ratios and combinations of the eigenvalues.

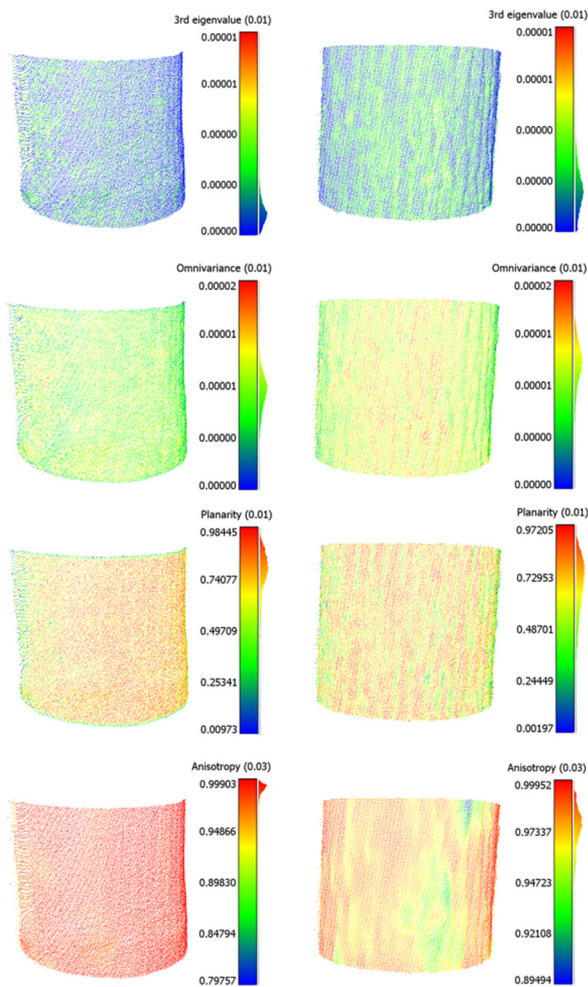


**Figure 4** Visualisation of geometric features on smooth versus rough bark. Left: European beech (tree height: 26.9 m, DBH: 47.2 cm), right: Pedunculate oak (tree height: 28.9 m, DBH: 39.9 cm). The patterns detected by geometric features are clearly visible. The histogram shows a more condensed distribution on the left, where bark is smoother

Exemplary results can be found in Figure 4. The shown beech is one of the largest ones in the data set, while the displayed oak is a relatively small individual. They were chosen as representatives due to their similar DBH and to show that the metrics provide stable results.

## 2.4.2 Filtering of Features

Each point of the extracted stem section is equipped with 33 scalar features at this stage – three eigenvalues and eight geometric features across three radii. These need to be condensed into conclusive single values per tree, to be used for tree species classification. To avoid distortion by undetected outliers, each eigenvalue is passed through an Interquartile Range (IQR) filter first that utilizes a coefficient of 2.5 times the interquartile range. Rough bark structure is represented by a large range in values, unlike evenly textured bark with little deviation. This filter was implemented to act as softly as possible, to avoid any occurring outliers without losing information. In case the IQR threshold acts too harshly and more than 80% of points in total are eliminated, instead all points are kept, since the final summary metrics are hardly influenced by outliers.

The filtered features are then condensed into values using eight summarizing metrics aiming at capturing their range and distribution. Specifically, these include the mean, median, absolute difference between mean and median, standard deviation, coefficient of variation, upper quartile, lower quartile, and interquartile range. Robust statistics were chosen to mitigate the influence of outliers caused by residual branches, occlusions, and local noise. In total, this amounts to the very high amount of 264 experimental, but representative features per tree. While all these values were initially calculated, not all were used later on, as certain geometric values and metrics appeared non-informative.

## 2.5 Feature Selection Strategy

Feature selection was guided by the most challenging class pair (hornbeam vs. beech). It consists of two steps: Initial, visual feature screening and automatic hierarchical clustering.

By visually inspecting linear scatter plots of all derived features and qualitatively comparing scalar field visualizations on smooth (e.g. European beech) and rough (e.g. European hornbeam, Pedunculate oak) bark across varying point densities, an initial manual pre-selection was performed. Features were retained if they exhibited reduced overlap between European beech and European hornbeam in

feature space and showed plausible contrasts in value range between smooth and fissured bark surfaces.

While this pre-selection is inherently empirical, it was intentionally conservative and aimed at removing only features that consistently failed to exhibit separability across species and scales.

As many features are either based on similar metrics, show similar effects or share the same computation radius, correlation needs to be considered. In order to reduce redundancy and maximize information, hierarchical clustering based on the absolute Spearman correlation was applied. Features were grouped using a distance threshold of 0.20, corresponding to a correlation of  $|p| > 0.80$ .

### 3 Results

#### 3.1 Stem Extraction Performance

From the total of 818 trees within the study area, 683 were assigned a DBH with center coordinate. Stem segments were successfully extracted from 536, yielding a success rate of almost 80%. Failures were primarily caused by three factors: errors in the DBH coordinate (12 cases), an overly aggressive density filter (12 cases) and the application of a minimum threshold, requiring at least 1000 points to remain after filtering (117 cases). The failed processing of six trees was not caught by the given exceptions. Overall, this indicates that the presented method of stem extraction can handle various resolutions, point densities and levels of noise or branch residuals. Selective visual inspection of the resulting stem section confirms this assessment.

**Table 1** Tree inventory metrics. The metrics were computed after stem extraction, geometric feature computation and metric computation on a total of 422 trees

	Oak	Beech	Hornbeam
n before	75 trees	344 trees	97 trees
n after	69 trees	277 trees	76 trees
height mean	28.8	21.7	20.2
± SD [m]	± 3.8	± 6.0	± 4.9
height min-max [m]	14.4-33.6	5.9-34.5	7.3-29.2
DBH mean	60.2 ± 17.1	27.7 ± 16.2	20.8 ± 9.8
± SD [cm]			
DBH min-max [cm]	13.0-100.9	6.2-97.6	8.0-45.7

### 3.2 Feature Selection

#### 3.2.1 Feature Completeness

Only trees with a full set of bark-derived features were included in the subsequent analysis. Incomplete feature vectors can be caused by mathematical errors due to division by very small eigenvalues. After this filtering step, 422 trees remained (see Tab. 1).

#### 3.2.2 Feature Reduction and Retained Feature Sets

The exploratory feature screening resulted in a major reduction revolving around  $\lambda_2$ ,  $\lambda_3$  and the largest neighborhood radius,  $r = 5$  cm. The eigenvalues as well as corresponding features were dropped as they contained little discriminative information.

This led to an initial feature set including  $\lambda_1$ , omnivariance as a measure of overall local point dispersion, anisotropy as an indicator of directional dominance in the point distribution, surface variation as a proxy for local roughness, and sphericity as a measure of isotropic versus elongated structure. The largest neighborhood radius (5 cm) was also excluded, as for beech and hornbeam trees with average DBHs of approximately 20 cm, a neighborhood of 10 cm diameter captures overall stem geometry rather than bark structure. This resulted in a total of 80 features.

The hierarchical clustering retained metrics targeting variability (e.g. quartiles and mean–median differences) and features from both 1 cm and 3 cm radii.

The hierarchical clustering concentrated the data frame to the following eight features:

- Upper quartile, surface variance,  $r = 1$  cm
- IQR, anisotropy,  $r = 1$  cm
- IQR, omnivariance,  $r = 1$  cm
- Upper quartile, omnivariance,  $r = 3$  cm
- $|\text{mean} - \text{median}|$ , anisotropy,  $r = 3$  cm
- Coefficient of variance,  $\lambda_1$ ,  $r = 3$  cm
- $|\text{mean} - \text{median}|$ , omnivariance,  $r = 1$  cm
- $|\text{mean} - \text{median}|$ , omnivariance,  $r = 3$  cm

Figure 5 shows a 2D scatter plot alongside a corresponding heat map of the correlations and a histogram of each feature. The high correlation between surface variance and anisotropy in the top left corner is due to using the Pearson correlation instead of Spearman, which was used earlier on in hierarchical clustering. The scatterplots indicate that oak, characterized by the roughest bark texture, is separable from beech in the derived feature space.

Hornbeam exhibits a slight shift in feature space but shows substantial overlap with the beech datasets.

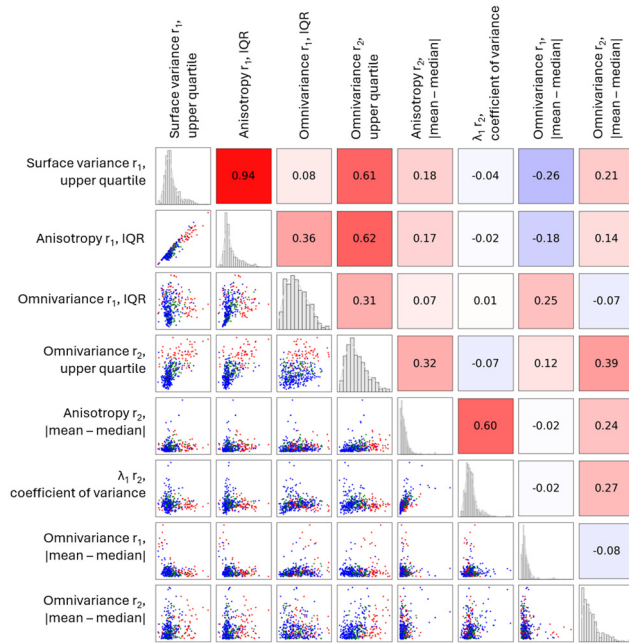


**Figure 5** Combined scatterplot–correlation matrix illustrating pairwise relationships between selected features. Two-dimensional scatter plots are shown in the lower triangular matrix, Pearson correlation coefficients are visualized as a heatmap in the upper triangular matrix, and univariate feature distributions are displayed along the main diagonal. Hornbeam data points are colored green, beech blue, oak red.  $r_1=0.1$  cm,  $r_2=0.3$  cm

## 4 Discussion

This contribution presents an end-to-end workflow for deriving bark-related features, starting with TLS point clouds of individual trees and ending with a selection of geometry-based bark features for every processed data set. The processing steps include stem extraction, computation of bark descriptors, their aggregation into scalar metrics and a feature reduction. Both statistical relevance and biological plausibility indicate that these features can capture bark roughness. This is shown by the clear distinct feature space of oak and beech in Figure 5. Usage is not limited to the three center species of this study and could be transferred to others.

However, the derived bark related features are highly sensitive to neighborhood radius and the scale of surface structure, which in turn depends on tree species and age. Uneven point cloud density further influences the stability of locally computed scalars.

Other approaches usually begin by fitting a cylinder into the stem and transferring the points to a planar projection. This allows for different metrics to be computed, such as surface deviation, projection into image form and image analysis or even stochastic analysis and Fourier transformation of the detected patterns. The choice against these approaches was once again founded in the heterogeneous point cloud qualities, as uniform point density and coverage could not be guaranteed across all trees. Additional information such as full-waveform profiles, intensity values or RGB was not available.

The European beech demonstrated stable, redundant features due to the large sample size and the morphological consistency of its smooth, even bark. The metrics clearly differ from those of the much more ridged, uneven oak. Restricting the analysis to only these two tree species serves as proof of concept and shows consistent and reliable performance. The European hornbeam, however, exhibits a clearly overlapping feature space with the European beech dataset. This underperformance may be due to the age of the trees, indicated by the low average DBH of 19 cm (approximately one third of the oaks' average DBH) with a standard deviation of 10 cm as well as the comparatively short average height of 20 m (see Table 1). As hornbeam takes several years to develop pronounced bark fissures, it is plausible that the trees chosen for this analysis are underdeveloped for the task.

The uneven class distribution lacked stable representativeness of the European hornbeam, as more samples might have supported the classification task. Result quality is also influenced by the sensitivity of the derived features to neighborhood size, their dependence on local point density and the potential bias introduced by feature reduction and feature importance methods.

TLS enables the development and validation of bark-scale geometric features, even though large-scale operational deployment will require adaptation to mobile and airborne platforms. The method's transferability to these sensor platforms is limited under the current state of art but may improve as sensors and registration advance to capture the fine-scale texture required for this approach.

In summary, this work demonstrates that bark-derived geometric descriptors can act as a complementary information source for automated forest inventories, particularly in situations where conventional structural features are insufficient to distinguish morphologically similar tree species.

Future work may include alternative bark parametrizations such as cylindrical unwrapping and surface

fitting, more extensive feature selection strategies as well as the use of machine learning classifiers. Probabilistic decision boundaries might work better than rigid class distinctions due to the overlapping feature distribution. With respect to the persisting difficulty of distinguishing European hornbeam and beech, complementary approaches such as temporal differences – e.g. differences in leaf retention – or species-specific microclimatic and soil conditions could be explored.

## References

- Bienert, A., Georgi, L., Kunz, M., von Oheimb, G., & Maas, H.-G. (2021). Automatic extraction and measurement of individual trees from mobile laser scanning point clouds of forests. *Annals of Botany*, 128(6), 787–804. <https://doi.org/10.1093/aob/mcab087>
- Damaševičius, R., Mozgeris, G., Kurti, A., & Maskeliūnas, R. (2024). Digital transformation of the future of forestry: an exploration of key concepts in the principles behind Forest 4.0. *Frontiers in Forests and Global Change*, 7, 1424327. <https://doi.org/10.3389/ffgc.2024.1424327>
- Ehrlich-Sommer, F., Hoenigsberger, F., Gollob, C., Nothdurft, A., Stampfer, K., & Holzinger, A. (2024). Sensors for Digital Transformation in Smart Forestry. *Sensors*, 24(3), 798. <https://doi.org/10.3390/s24030798>
- Hackel, T., Wegner, J. D., & Schindler, K. (2016). Contour Detection in Unstructured 3D Point Clouds. 2016 IEEE Conference on Computer Vision and Pattern Recognition (CVPR), Las Vegas, NV, USA, 2016, 1610–1618. <https://doi.org/10.1109/CVPR.2016.178>
- Koenig, K., & Höfle, B. (2016). Full-waveform airborne laser scanning in vegetation studies – a review of point cloud and waveform features for tree species classification. *Forests*, 7(9), 198. <https://doi.org/10.3390/f7090198>
- Li, J., Hu, B., & Noland, T. L. (2013). Classification of tree species based on structural features derived from high density LiDAR data. *Agricultural and Forest Meteorology*, 171, 104–114. <https://doi.org/10.1016/j.agrformet.2012.11.012>
- Liang, X., Kankare, V., Hyypä, J., Wang, Y., Kukko, A., Haggrén, H., Yu, X., Kaartinen, H., Jaakkola, A., Guan, F., Holopainen, M., & Vastaranta, M. (2016). Terrestrial laser scanning in forest inventories. *ISPRS Journal of Photogrammetry and Remote Sensing*, 115, 63–77. <https://doi.org/10.1016/j.isprsjprs.2016.01.006>
- Mahabir, R., & Shrestha, R. M. (2015). Climate change and forest management: Adaptation of geospatial technologies. *IEEE Fourth International Conference on Agro-Geoinformatics (Agro-geoinformatics)*, 209–214. <https://doi.org/10.1109/Agro-Geoinformatics.2015.7248108>
- Meng, Y., Dong, X., Han, K., Liu, H., Qu, H., & Gao, T. (2024). Classification of Tree Species Using Point Cloud Features from Terrestrial Laser Scanning. *Forests*, 15(12), 2110. <https://doi.org/10.3390/f15122110>
- Michałowska, M., & Rapiński, J. (2021). A review of tree species classification based on airborne LiDAR data and applied classifiers. *Remote Sensing*, 13(3), 353. <https://doi.org/10.3390/rs13030353>
- Morin, X., Fahse, L., Jactel, H., Scherer-Lorenzen, M., García-Valdés, R., & Bugmann, H. (2018). Long-term response of forest productivity to climate change is mostly driven by change in tree species composition. *Scientific Reports*, 8(1), 5627. <https://doi.org/10.1038/s41598-018-23763-y>
- Wang, G. G., Lu, D., Gao, T., Zhang, J., Sun, Y., Teng, D., & Zhu, J. (2024). Climate-smart forestry: An AI-enabled sustainable forest management solution for climate change adaptation and mitigation. *Journal of Forestry Research*, 36(1), 7. <https://doi.org/10.1007/s11676-024-01802-x>
- Weinmann, M., Jutzi, B., Hinz, S., & Mallet, C. (2015). Semantic point cloud interpretation based on optimal neighborhoods, relevant features and efficient classifiers. *ISPRS Journal of Photogrammetry and Remote Sensing*, 105, 286–304. <https://doi.org/10.1016/j.isprsjprs.2015.01.016>